

# The white dwarf in AE Aqr brakes harder

Christopher W. Mauche\*

*Lawrence Livermore National Laboratory, L-473, 7000 East Avenue, Livermore, CA 94550*

Accepted 2006 April 13. Received 2006 April 12; in original form 2005 December 12

## ABSTRACT

Taking advantage of the very precise de Jager et al. optical white dwarf orbit and spin ephemerides; *ASCA*, *XMM-Newton*, and *Chandra* X-ray observations spread over 10 yrs; and a cumulative 27 yr baseline, we have found that in recent years the white dwarf in AE Aqr is spinning down at a rate that is slightly faster than predicted by the de Jager et al. spin ephemeris. At the present time, the observed period evolution is consistent with either a cubic term in the spin ephemeris with  $\dot{P} = 3.46(56) \times 10^{-19} \text{ d}^{-1}$ , which is inconsistent in sign and magnitude with magnetic-dipole radiation losses, or an additional quadratic term with  $\dot{P} = 2.0(1.0) \times 10^{-15} \text{ d d}^{-1}$ , which is consistent with a modest increase in the accretion torques spinning down the white dwarf. Regular monitoring, in the optical, ultraviolet, and/or X-rays, is required to track the evolution of the spin period of the white dwarf in AE Aqr.

**Key words:** binaries: close – stars: individual (AE Aqr) – novae, cataclysmic variables – stars: rotation – white dwarfs.

## 1 INTRODUCTION

AE Aqr is a bright ( $V \approx 11$ ), nova-like cataclysmic binary consisting of a magnetic white dwarf primary and a K4–5 V secondary with a long 9.88 hr orbital period and the shortest known white dwarf spin period  $P = 33.08 \text{ s}$  (Patterson 1979). Although originally classified and interpreted as a disk-accreting DQ Her star (Patterson 1994), AE Aqr displays a number of unusual features that are not naturally explained by this model. First, violent flaring activity is observed in the radio, optical, ultraviolet, X-ray, and TeV  $\gamma$ -rays. Second, the Balmer emission lines are single peaked and produce Doppler tomograms that are not consistent with those of an accretion disk. Third, the white dwarf is spinning down at a rate  $\dot{P} = 5.64 \times 10^{-14} \text{ s s}^{-1}$  (de Jager et al. 1994, hereafter, de Jager). Although this corresponds to the small rate of change of  $1.78 \text{ ns yr}^{-1}$ , AE Aqr’s spin-down is typically characterized as “rapid” because the characteristic time  $P/\dot{P} \approx 2 \times 10^7 \text{ yr}$ , which is short compared to the lifetime of the binary, and because the spin-down luminosity  $L_{\text{sd}} = -I\Omega\dot{\Omega} \approx 1 \times 10^{34} \text{ erg s}^{-1}$  (where  $I \approx 0.2M_{\text{wd}}R_{\text{wd}}^2 \approx 2 \times 10^{50} \text{ g cm}^2$  is the white dwarf moment of inertia,  $M_{\text{wd}}$  and  $R_{\text{wd}}$  are the white dwarf mass and radius, respectively,  $\Omega = 2\pi/P$ , and  $\dot{\Omega} = -2\pi\dot{P}/P^2$ ), which exceeds the secondary’s thermonuclear luminosity by an order of magnitude and the accretion luminosity by two

orders of magnitude. Given this, AE Aqr could be thought of as being powered primarily by the ultimate in clean energy sources: a flywheel.

Because of its unique properties and variable emission across the electromagnetic spectrum, AE Aqr has been the subject of numerous studies, including an intensive multiwavelength observing campaign in 1993 October (Casares et al. 1996, and the series of papers in ASPC 85). Based on these studies, AE Aqr is now widely believed to be a former supersoft X-ray binary (Schenker et al. 2002) and current *magnetic propeller* (Wynn, King, & Horne 1997), with most of the mass lost by the secondary being flung out of the binary by the magnetic field of the rapidly rotating white dwarf. These models explain many of AE Aqr’s unique characteristics, including the fast spin rate and rapid secular spin-down rate of the white dwarf, the anomalous spectral type of the secondary, the anomalous C to N abundance (Mauche, Lee, & Kallman 1997), the absence of signatures of an accretion disk (Welsh, Horne, & Gomer 1998), the violent flaring activity (Pearson, Horne, & Skidmore 2003), and the origin of the radio and TeV  $\gamma$ -ray emission (Kuijpers et al. 1997; Meintjes & Venter 2003).

To build on this observational and theoretical work, while taking advantage of a number of improvements in observing capabilities, during 2005 August 28–September 2 a group of professional and amateur astronomers conducted a campaign of multiwavelength (radio, optical, ultraviolet, X-ray, and TeV  $\gamma$ -ray) observations of AE Aqr. Analyses of

\* E-mail: mauche@cygnus.llnl.gov

these data are ongoing, but here we present a fundamental result – the spin period of the white dwarf – that relies solely on photometric data from the *Chandra X-ray Observatory* and archival data from *ASCA* and *XMM-Newton*.

## 2 OBSERVATIONS AND ANALYSIS

AE Aqr was observed by *ASCA* with the Gas Imaging Spectrometer (GIS) detectors and the Solid-State Imaging Spectrometer (SIS) detectors beginning on 1995 October 14 at 00:16 UT for 82 ks (Sequence Number 33005000), by *XMM* with the European Photon Imaging Collaboration (EPIC) pn CCD detector beginning on 2001 November 7 at 23:47 UT for 14 ks (ObsID 0111180201), and by *Chandra* with the High-Energy Transmission Grating (HETG) and the Advanced CCD Imaging Spectrometer (ACIS) detector beginning on 2005 August 30 at 06:37 UT for 81 ks (ObsID 5431). The *ASCA* and *XMM* data have been previously discussed by Eracleous (1999); Choi, Dotani, & Agrawal (1999); Osborne [2002, unpublished presentation at the Third Magnetic Cataclysmic Variable Workshop (IAU Coll. 190)]; and Itoh et al. (2006).

The *ASCA* and *XMM* data and the *Chandra* data were extracted from the High Energy Astrophysics Science Archive Research Center and the *Chandra* Data Archive, respectively. The data files used for subsequent analysis were the *ASCA* GIS and SIS screened bright mode event files, the *XMM* EPIC pn pipeline processed event file, and the *Chandra* level 2 pipeline processed event file. The data in these files were manipulated as follows. First, all times were converted from spacecraft time to Terrestrial Time (TT) and corrected to the solar system barycenter using the *ASCA* FTOOLS<sup>1</sup> v6.0 tool `timeconv`, the *XMM* Science Analysis Software (SAS<sup>2</sup>) v6.5.0 tool `barycen`, and the *Chandra* Interactive Analysis of Observations (CIAO<sup>3</sup>) v3.2 tool `axbary`. The barycentric corrections produced by these different software packages were checked against those of the Interactive Data Language (IDL) procedure `barycen`<sup>4</sup> (which does not by default account for the varying light travel time between the satellite and the center of Earth), and were found to agree within 40, 210, and 200 ms for *ASCA*, *XMM*, and *Chandra*, respectively, consistent with the size of each satellite's orbit. Second, source and background events were extracted from the event files using custom IDL software. For *Chandra*, events were collected from the zeroth order image and the  $\pm$  first order dispersed spectrum using the region masks in the level 2 pha file. Third, event times  $t$  were converted to white dwarf orbit and spin phases via the relations  $\phi_{\text{orb}} = \Omega_{\text{orb}}(t - T_0)$  and  $\phi_{\text{spin}} = \Omega_0(t - T_{\text{max}}) + \frac{1}{2}\dot{\Omega}(t - T_{\text{max}})^2$ , respectively, where  $\Omega_{\text{orb}} = 2\pi/P_{\text{orb}}$ ,  $\Omega_0 = 2\pi/P_{33}$ , and  $\dot{\Omega} = -2\pi\dot{P}_{33}/P_{33}^2$  and  $T_0$ ,  $P_{\text{orb}}$ ,  $T_{\text{max}}$  (BJD)  $\approx 2445172$ ,  $P_{33} = 0.00038283263840$  d, and  $\dot{P}_{33} = 5.642 \times 10^{-14}$  d d<sup>-1</sup> are the white dwarf orbit and

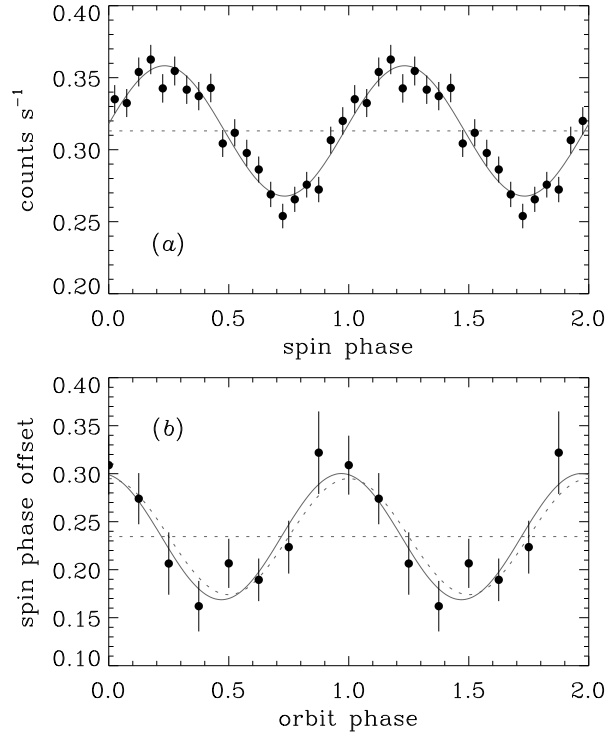


**Figure 1.** (a) *Chandra* spin phase folded count rate light curve of AE Aqr (filled circles with error bars), best-fitting cosine (solid curve), and mean count rate  $A$  (dotted line). (b) Spin phase offset as a function of orbit phase (filled circles with error bars), best-fitting cosine (solid curve), mean phase offset (dotted line), and the predicted spin phase offset variation for the de Jager white dwarf orbit ephemeris and a pulse time delay of 2 s (dotted curve).

spin ephemeris constants from Table 4 of de Jager.<sup>5</sup> Fourth, filters were applied to restrict attention to events from two orbital cycles for *ASCA* and *Chandra* and  $\frac{3}{8}$  of an orbital cycle centered on  $\phi_{\text{orb}} = 0.25$  for *XMM*. The resulting range of orbit phases and observation dates are listed in Table 1. Fifth, background-subtracted spin phase folded count rate light curves were calculated and fit with the cosine function  $A + B \cos(\phi_{\text{spin}} - \phi_0)$ , where  $A$  is the mean count rate,  $B$  is the pulse semiamplitude, and  $\phi_0$  is the phase offset (expressed in cycles  $\phi_0/2\pi$  in what follows). Given that the optical, ultraviolet, and X-ray spin pulses are aligned in phase (Patterson et al. 1980; Eracleous et al. 1995),  $\phi_0$  should be equal to zero to within the uncertainty of the de Jager spin ephemeris, if the ephemeris remains valid at the times of the *ASCA*, *XMM*, and *Chandra* observations.

<sup>1</sup> Available at <http://heasarc.gsfc.nasa.gov/docs/software/lheasoft/ftools>. Note that the expression in §6 of de Jager for the times of spin

<sup>2</sup> Available at <http://xmm.vilspa.esa.es/sas/>.

<sup>3</sup> Available at <http://cxc.harvard.edu/ciao/>.

<sup>4</sup> Available at <http://astro.uni-tuebingen.de/software/idl/aitlib/astro/>.  $2 \times 10^{-5}$  cycles at the time of the *Chandra* observation.

**Table 1.** Log of observations.

Satellite	Orbit Phase $\phi_{\text{orb}}$ (cycles)	Date [BJD(TT) – 2400000]
<i>ASCA</i>	11738.8000–11740.8000	50004.62127–50005.44459
<i>XMM</i>	17124.0625–17124.4375	52221.49479–52221.64916
<i>Chandra</i>	20504.0000–20506.0000	53612.86503–53613.68834

## 2.1 *Chandra* results, ignoring the pulse time delays

We begin the analysis by considering the *Chandra* data, which covers two full binary orbits of AE Aqr without interruption by Earth occultations or detector shutdowns. As shown in the top panel of Figure 1, the *Chandra* background-subtracted spin phase folded count rate light curve of AE Aqr is reasonably well fit ( $\chi^2_\nu = 19.1/17 = 1.12$ ) by the cosine function with a mean count rate  $A = 0.313 \pm 0.002$  counts  $\text{s}^{-1}$ , a relative amplitude  $B/A = 15 \pm 1$  per cent, and a phase offset  $\phi_0 = 0.232 \pm 0.011$  cycles (throughout the paper, errors are  $1\sigma$  or 68 per cent confidence for 1 degree of freedom); the phase offset differs from the de Jager spin ephemeris by  $4.4\sigma$ . To check if this result is affected by intensity variations around the orbit, we repeated the above procedure for each of 8 contiguous orbit phase intervals centered on  $\phi_{\text{orb}} = [0, 1, 2, \dots, 7]/8$ . The resulting variation of the spin phase offset with orbit phase is shown in the bottom panel of Figure 1 and is well fit ( $\chi^2_\nu = 4.31/5 = 0.86$ ) by the cosine function  $A' + B' \cos(\phi_{\text{orb}} - \phi'_0)$ , with  $A' = 0.234 \pm 0.010$  spin cycles,  $B' = 0.066 \pm 0.015$  spin cycles, and  $\phi'_0 = -0.03 \pm 0.03$  orbit cycles: the orbit phase offset  $\phi'_0$  is consistent with zero, the mean spin phase offset  $A'$  is consistent with the value derived above for  $\phi_0$ , and the semiamplitude  $B'$  corresponds to a pulse time delay  $B'P_{33} = 2.17 \pm 0.48$  s, which is consistent with that measured in the optical ( $2.04 \pm 0.13$  s, de Jager) and ultraviolet ( $1.93 \pm 0.03$  s, Eracleous et al. 1994). From this result,<sup>6</sup> we conclude that the source of the pulsating X-rays follows the motion of the white dwarf as it orbits around the center of mass in AE Aqr.

## 2.2 *ASCA*, *XMM*, and *Chandra* results, accounting for the pulse time delays

Given these results, we analyzed the *ASCA*, *XMM*, and *Chandra* data for AE Aqr assuming that in each case the X-ray source follows the motion of the white dwarf. Specifically, we corrected the barycentric event times by  $2 \cos(\phi_{\text{orb}})$  s before calculating the spin phases, the spin phase folded light curves, and the cosine fit parameters. The pulse time delay correction allows us to use all the data for each observation, without regard to gaps due to Earth occultations or

detector shutdowns (*ASCA*) or to the varying source intensity (all three observations). With the pulse time delay corrections and the previous orbit phase filters, the spin phase folded count rate light curves and the best-fitting cosines are as shown in Figure 2 and the best-fitting cosine parameters and the Barycentric Julian Dates of the X-ray pulse maxima are as listed in Table 2. Figure 3 plots the phase offsets versus time, demonstrating that the observed phases  $O$  are diverging from the calculated phases  $C$  assuming the de Jager spin ephemeris: accounting for the error in the ephemeris, the two differ by  $1.7\sigma$ ,  $3.9\sigma$ , and  $4.4\sigma$  for *ASCA*, *XMM*, and *Chandra*, respectively. Apparently, the white dwarf in AE Aqr is slowly but progressively “coming off the rails” of the de Jager spin ephemeris.

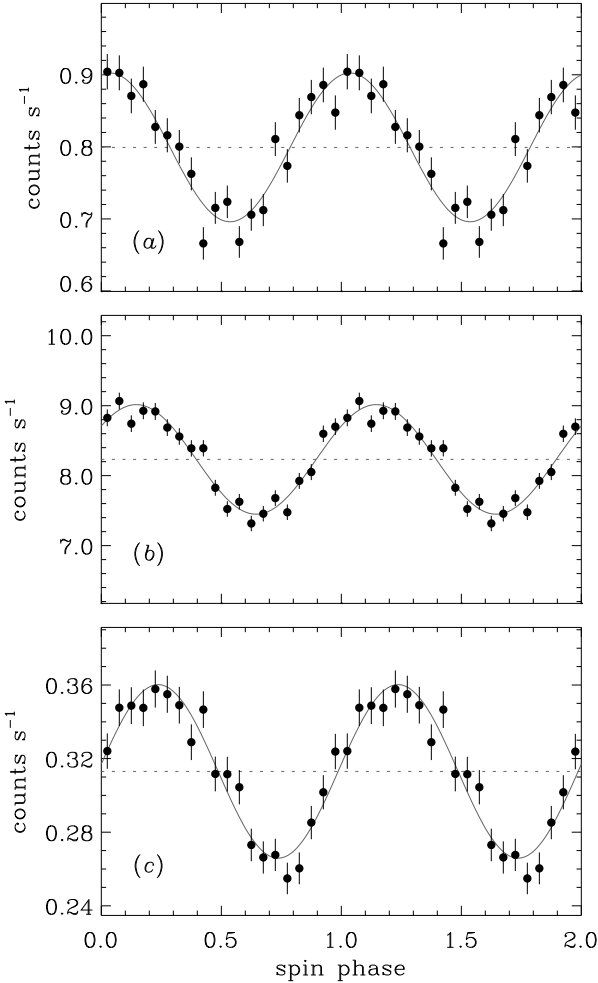
## 3 UPDATING THE AE AQR WHITE DWARF SPIN EPHEMERIS

The trend displayed in Figure 3 of the difference between the observed and calculated AE Aqr white dwarf spin phases is steeper than can be explained by an increase in either the value of the  $\dot{P}_{33}$  parameter or the size of the parameter uncertainties in the de Jager spin ephemeris. Given the limited baseline and the limited amount of X-ray data, the observed trend is consistent with the addition to the ephemeris of either a  $\ddot{P}_{33}$  term centered on  $T_{\text{max}}$  or an additional  $\dot{P}_{33}$  term centered on a late date  $T'_{\text{max}}$ . In the first case, the Taylor expansion of the spin frequency  $\Omega(t) = \Omega_0 + \dot{\Omega}(t - T_{\text{max}}) + \frac{1}{2}\ddot{\Omega}(t - T_{\text{max}})^2$  results in a cubic term in the expansion for  $\phi_{\text{spin}} = \Omega_0(t - T_{\text{max}}) + \frac{1}{2}\dot{\Omega}(t - T_{\text{max}})^2 + \frac{1}{6}\ddot{\Omega}(t - T_{\text{max}})^3$  (Manchester & Taylor 1977), so  $O - C = -\frac{1}{6}\ddot{\Omega}(t - T_{\text{max}})^3$  and the optical and X-ray data are consistent with  $\ddot{\Omega} = -1.48(24) \times 10^{-11} \text{ d}^{-3}$  or  $\dot{P}_{33} = 3.46(56) \times 10^{-19} \text{ d}^{-1}$ . In the second case,  $O - C = -\frac{1}{2}\dot{\Omega}'(t - T'_{\text{max}})^2$  and the X-ray data are consistent with  $T'_{\text{max}}(\text{BJD}) = 2447650 \pm 1200$  and  $\dot{\Omega}' = -8.5(4.4) \times 10^{-8} \text{ d}^{-2}$  or  $\dot{P}'_{33} = 2.0(1.0) \times 10^{-15} \text{ d d}^{-1}$ . (In both cases, the quoted errors account for the error in the de Jager spin ephemeris.) Of the two options, the quadratic fit is preferred, since it provides a slightly better fit to the data and produces phase residuals that are smaller ( $\leq 0.07$  cycles for the quadratic term compared to  $\leq 0.13$  for the cubic term) during the epoch studied by de Jager (1978.5–1992.6). In either case, the frequency derivatives are negative and the period derivatives are positive, so during the epoch covered by the *ASCA*, *XMM*, and *Chandra* X-ray observations (1995.8–2005.7), the white dwarf in AE Aqr was braking (slightly) harder than described by the de Jager spin ephemeris.

<sup>6</sup> Reinsch et al. (1995) previously reported that the *ROSAT* X-ray pulse time delays vary with the orbital period and are in phase with the optical/ultraviolet pulse time delays, but they did not provide details.

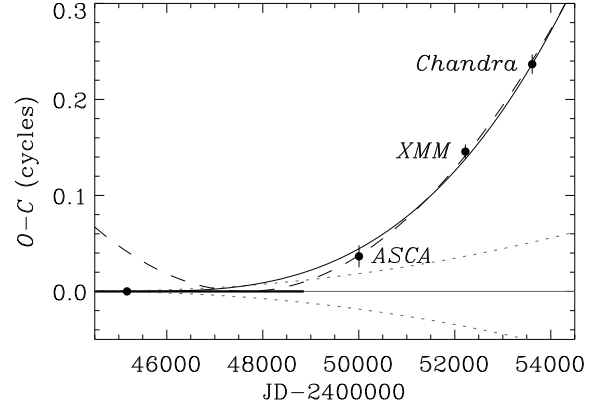
**Table 2.** Best-fitting cosine parameters  $A + B \cos(\phi_{\text{spin}} - \phi_0)$ .

Satellite	$\chi^2_\nu$	$A$ (counts s <sup>-1</sup> )	$B$ (counts s <sup>-1</sup> )	$B/A$	$\phi_0$ (rel. cycles)	Date of pulse maximum [BJD(TT) - 2400000]
<i>ASCA</i>	1.43	$0.799 \pm 0.005$	$0.103 \pm 0.007$	$0.129 \pm 0.009$	$0.037 \pm 0.011$	$50004.7037529 \pm 0.0000044$
<i>XMM</i>	1.66	$8.232 \pm 0.026$	$0.783 \pm 0.037$	$0.095 \pm 0.004$	$0.146 \pm 0.007$	$52221.5720142 \pm 0.0000029$
<i>Chandra</i>	1.09	$0.313 \pm 0.002$	$0.047 \pm 0.003$	$0.151 \pm 0.009$	$0.237 \pm 0.010$	$53613.2767058 \pm 0.0000039$

**Figure 2.** (a) *ASCA*, (b) *XMM*, and (c) *Chandra* spin phase folded count rate light curves of AE Aqr (filled circles with error bars), best-fitting cosines (solid curves), and mean count rates  $A$  (dotted lines). Each panel is scaled to  $\pm 25$  per cent of the mean count rate.

#### 4 DISCUSSION

Taking advantage of the very precise de Jager optical white dwarf orbit and spin ephemerides; *ASCA*, *XMM*, and *Chandra* X-ray observations spread over 10 yrs; and a cumulative 27 yr baseline, we have found that in recent years the white dwarf in AE Aqr is spinning down at a rate that is slightly faster than predicted by the de Jager spin ephemeris. At

**Figure 3.** Observed minus calculated spin phases of AE Aqr as a function of time (filled circles with error bars), the  $1\sigma$  error envelope of the de Jager spin ephemeris (dotted curves), the cubic fit to the de Jager optical datum and the *ASCA*, *XMM*, and *Chandra* X-ray data (solid curve), and the quadratic fit to the X-ray data (dashed curve). The epoch studied by de Jager is indicated by the thick horizontal line.

the present time, the observed period evolution is consistent with either a cubic term in the spin ephemeris with  $\ddot{P}_{33} = 3.46(56) \times 10^{-19} \text{ d}^{-1}$  centered on  $T_{\text{max}}$  or an additional quadratic term with  $\dot{P}'_{33} = 2.0(1.0) \times 10^{-15} \text{ d d}^{-1}$  centered on  $T'_{\text{max}}(\text{BJD}) = 2447650 \pm 1200$ . We consider the implications of each option in turn.

If the observed  $O - C$  residuals are due to a cubic term in the spin ephemeris, it is possible to make an interesting comparison between the AE Aqr white dwarf X-ray pulsar and neutron star radio pulsars. In a vacuum, a rotating star with a misaligned magnetic dipole loses rotational kinetic energy via magnetic-dipole radiation at a rate  $L_{\text{sd}} = -I\Omega\dot{\Omega} = 2\mu^2 \sin^2 \theta \Omega^4 / 3c^3$ , where  $\mu = BR^3$  is the magnetic moment,  $B$  is the surface magnetic field strength,  $R$  is the stellar radius, and  $\theta$  is the angle between the rotation and magnetic axes. It is convenient to express this as  $\dot{\Omega} = -K\Omega^n$  with  $K = 2\mu^2 \sin^2 \theta / 3Ic^3$  and the so-called braking index  $n = 3$ . Ignoring the fact that the white dwarf in AE Aqr is not isolated [the light cylinder radius ( $r_{\text{lc}} = c/\Omega = 1.6 \times 10^{11} \text{ cm}$ ) is comparable to the binary separation ( $a \approx 2 \times 10^{11} \text{ cm}$ ), so the white dwarf magnetic field will drag against the secondary, the magnetic field of the secondary, and the mass lost by the secondary], if one assumes that the observed spin-down is due solely to magnetic-dipole radiation losses, one obtains that  $\mu \approx 1 \times 10^{34} \text{ G cm}^3$  or  $B \sim 50 \text{ MG}$  (Ikhsanov 1998), compa-

rable to that observed in polars. However, one also obtains  $\dot{\Omega} = n\dot{\Omega}^2/\Omega = 1.07 \times 10^{-15} \text{ d}^{-3}$  or  $\dot{P} = -8.40 \times 10^{-24} \text{ d}^{-1}$ , which results is a *decrease* in  $O - C$  by 0.1 cycles in  $10^5$  yrs, while we have observed an *increase* in  $O - C$  by 0.24 cycles in 27 yrs. Expressed another way, we have derived not  $n = 3$  but  $n \approx -42000$ . Clearly, the enhanced spin-down of the white dwarf in AE Aqr has nothing to do with magnetic-dipole radiation losses. On the other hand, if the observed  $O - C$  residuals are due to an additional quadratic term in the spin ephemeris, the spin-down rate is a modest  $3.5 \pm 1.8$  per cent greater than the rate derived by de Jager, which easily could be accommodated by, e.g., a small increase in the mass transfer rate from the secondary, leading to an enhanced spin-down torque on the white dwarf.

While we have found that additional low-order terms in the Taylor series expansion of the white dwarf spin ephemeris adequately fit the trend of the  $O - C$  residuals of the *ASCA*, *XMM*, and *Chandra* X-ray light curves of AE Aqr, providing independent evidence of the nominal validity of the de Jager ephemerides, we caution that our results are based on only three data points spread over 10 yrs. First, it is possible that the spin evolution of AE Aqr is more complex than assumed, that  $O - C$  varies on shorter timescales and manifests larger excursions than sampled, and that the good quadratic and cubic fits to the  $O - C$  residuals of the X-ray data are fortuitous. Second, the quadratic and cubic spin ephemerides of §3 should be used with caution, since they have yet to be shown to have any *predictive* capability. Regular monitoring, in the optical, ultraviolet, and/or X-rays, is required to track the evolution of the AE Aqr pulse period, to determine if the white dwarf continues to spin down at the current rate, or if (as seems likely) it varies stochastically in response to changes in the mass-transfer rate, the varying efficiency of the magnetic propeller (e.g., the fraction of the mass-transfer rate that is expelled from the binary versus that accreted by the white dwarf), etc.

## ACKNOWLEDGMENTS

The author is pleased to acknowledge Okkie de Jager for an educational and entertaining exchange of e-mails, Koji Mukai for resolving a problem with the *ASCA* FTOOL `barycen`, Mike Arida for help installing the *XMM* SAS, and Klaus Reinsch, Bill Welsh, Nazar Ikhsanov, and the anonymous referee for information, comments, and suggestions that improved the quality and clarity of this manuscript. This research made use of *ASCA* and *XMM* data obtained from the High Energy Astrophysics Science Archive Research Center (HEASARC), provided by NASA's Goddard Space Flight Center. Support for this work was provided by NASA through *Chandra* Award Number GO5-6020X issued by the *Chandra X-ray Observatory* Center, which is operated by the Smithsonian Astrophysical Observatory for and on behalf of NASA under contract NAS8-03060. This work was performed under the auspices of the U.S. Department of Energy by University of California, Lawrence Livermore National Laboratory under Contract W-7405-Eng-48.

## REFERENCES

- Casares J., Mouchet M., Martinez-Pais I. G., Harlaftis E. T., 1996, MNRAS, 282, 182  
 Choi C.-S., Dotani T., Agrawal P. C., 1999, ApJ, 525, 399  
 de Jager O. C., Meintjes P. J., O'Donoghue D., Robinson E. L., 1994, MNRAS, 267, 577  
 Eracleous M., 1999, ASPC, 157, 343  
 Eracleous M., Horne K., Osborne J. P., Clayton K. L., 1995, ASPC, 85, 392  
 Eracleous M., Horne K., Robinson E. L., Zhang E.-H., Marsh T. R., Wood J. H., 1994, ApJ, 433, 313  
 Ikhsanov N. R., 1998, A&A, 338, 521  
 Itoh, K., Okada, S., Ishida M., Kunieda, H., 2006, ApJ, 639, 397  
 Kuijpers J., Fletcher L., Abada-Simon M., Horne K. D., Raadu M. A., Ramsay G., Steeghs D., 1997, A&A, 322, 242  
 Manchester R. N., Taylor J. H., 1977, Pulsars (San Francisco: Freeman)  
 Mauche C. W., Lee Y. P., Kallman T. R., 1997, ApJ, 477, 832  
 Meintjes P. J., Venter L. A., 2003, MNRAS, 341, 891  
 Patterson J., 1979, ApJ, 234, 978  
 Patterson J., 1994, PASP, 106, 209  
 Patterson J., Branch D., Chincarini G., Robinson E. L., 1980, ApJ, 240, L133  
 Pearson K. J., Horne K., Skidmore W., 2003, MNRAS, 338, 1067  
 Reinsch K., Beuermann K., Hanusch H., Thomas H.-C., 1995, ASPC, 85, 115  
 Schenker K., King A. R., Kolb U., Wynn G. A., Zhang Z., 2002, MNRAS, 337, 1105  
 Welsh W. F., Horne K., Gomer R., 1998, MNRAS, 298, 285  
 Wynn G. A., King A. R., Horne K., 1997, MNRAS, 286, 436

This paper has been typeset from a  $\text{\TeX}$ / $\text{\LaTeX}$  file prepared by the author.